

R. Mateus et al.

Effects of Deuterium and Nitrogen Irradiation on Be-W Coatings Grown by TVA

(18th May 2015 – 22nd May 2015)
Aix-en-Provence, France

“This document is intended for publication in the open literature. It is made available on the clear understanding that it may not be further circulated and extracts or references may not be published prior to publication of the original when applicable, or without the consent of the Publications Officer, EUROfusion Programme Management Unit, Culham Science Centre, Abingdon, Oxon, OX14 3DB, UK or e-mail Publications.Officer@euro-fusion.org”.

“Enquiries about Copyright and reproduction should be addressed to the Publications Officer, EUROfusion Programme Management Unit, Culham Science Centre, Abingdon, Oxon, OX14 3DB, UK or e-mail Publications.Officer@euro-fusion.org”.

The contents of this preprint and all other EUROfusion Preprints, Reports and Conference Papers are available to view online free at <http://www.euro-fusionscipub.org>. This site has full search facilities and e-mail alert options. In the JET specific papers the diagrams contained within the PDFs on this site are hyperlinked.

Effects of deuterium and nitrogen irradiation on Be-W coatings grown by TVA

R Mateus^{1*}, N Catarino¹, M C Sequeira¹, E Alves¹, C Porosnicu², C P Lungu² and A Hakola³

¹*Instituto de Plasmas e Fusão Nuclear, Instituto Superior Técnico, Universidade de Lisboa, Av. Rovisco Pais, 1049-001, Lisboa, Portugal*

²*National Institute for Lasers, Plasma and Radiation Physics, Bucharest 077125, Romania*

³*VTT Technical Research Centre of Finland Ltd, VTT, Finland*

*E-mail: corresponding author e-mail address: rmateus@ipfn.ist.utl.pt

Abstract. (137 words)

(a total of 2140 words in the entire document)

Different Be:W samples presenting a wide range of compositions are being deposited by TVA and used as standards in order to investigate the retention mechanisms of deuterium and gas seeding impurities in mixed Be:W layers under irradiation. In this work energetic deuterium and nitrogen ions were implanted in a batch of these samples up to fluences of 5×10^{17} ions/cm² in order to evaluate the influence of stoichiometry in the retention mechanisms, being the induced chemical and structural changes evaluated by ion beam analysis, scanning electron microscopy, X-ray diffraction and photoelectron spectroscopies. The results seem to evidence that, besides the elemental composition, deuterium retention highly depends of the morphology of the exposed surfaces, and typically, the retention of nitrogen follows the content of beryllium. Nevertheless, the formation of tungsten nitride (β -W₂N) is always evident in the collected diffractograms.

1. Introduction (400 words)

The first wall of the international nuclear fusion experiment (ITER) will be covered by beryllium (Be), whereas tungsten (W) will be used as plasma facing material in the divertor module. Impurities eroded from the main wall will be transported and re-deposited mainly in the divertor region. The transport of impurities from the divertor to the primary wall will be mitigated by the magnetic field configuration. Nevertheless, it could be significant nearby the divertor area. A wide range of Be:W mixed compositions and deposition morphologies will be formed and will evolve over time during ITER operation, and it is a demand to investigate the consequences arising from these modifications. In particular, they will shape the retention mechanisms of deuterium (D) and seeding impurities as nitrogen (N) [1-5]. A huge number of relevant data relative to the irradiation of pure W and Be surfaces by D [1,2] and N [3,4] ions is already available in the community. It is time now to evaluate the retention mechanisms in mixed Be:W samples with standard compositions and this is the aim of the present work.

The use of high fluences in irradiation experiments may result in the fast saturation of the exposed surfaces, being the

thicknesses of the enriched layers comparable to the in-depth range of the impinging ions. This is the case for N^+ implantation, where a saturation threshold is reached quickly with the formation of stable nitride compositions due to the affinity of N to react with Be and W [3,4]. Two beryllium nitride phases with similar enthalpies of formation could be formed: cubic α - Be_3N_2 ($\Delta H_f = -589.9$ KJ/mol) and hexagonal β - Be_3N_2 (-572.0 KJ/mol) [6]. Similarly, two tungsten nitride phases are presented in the W-N binary system: hexagonal WN ($\Delta H_f = -24$ KJ/mol) [7] forms at temperatures up to ~ 600 K, and the β - W_2N (-72 KJ/mol) [7] is formed at higher temperatures [4]. It is reported the formation of Be_3N_2 [3] and WN [4] by implanting N ions at low temperature regimes in the energy ranges of 1.5-2.5 keV [3] and below 0.5 keV [4]. Higher implantation energies may lead to different results, while the interaction between the components depends of the kinetic energy of the impinging ions. In principal, N should react preferentially with Be because the enthalpies of formation for Be nitrides are significantly lower than for W nitrides. It will be interesting to compare their formation on mixed Be:W layers.

2. Experiment and methods (269 words)

Pure Be and W and mixed Be:W coatings with stoichiometric ratios of (5:5) and (1:9) were deposited by the thermionic vacuum arc (TVA) method [8] on mirror quality silicon plates with nominal thicknesses of 400 and 300 nm, and irradiated afterwards by 15 keV D^+ or 30 keV N^+ energetic ions with fluences of 1 and 5×10^{17} ions/cm², being the thicker layers used on the D^+ exposure. Previous simulations using the SRIM code [9] assure that at these incident energies all the implantation depth ranges remains within the Be:W layers.

It could be advantageous to carry out experiments with energetic ions, while they penetrate deeper in the exposed layers, leading to higher retention ratios and retarding the saturation of the coatings by D or N bombardment. Thicker implantation depth ranges are also extremely advantageous in X-ray diffraction (XRD) measurements for phase identification, especially because unit cells composed only by light elements induce weaker XRD patterns [10].

Before and after the implantation campaign, the coating thickness and the depth profiles for the heavier elements were analysed by Rutherford backscattering (RBS) using 2.2 MeV $^4He^+$ ion beams. For the analysis of Be, N and O depth profiles by RBS, 1.0 and 1.4 MeV H^+ ion beams were used in order to enhance the corresponding backscattering yields [11]. For D quantification by nuclear reaction analysis (NRA), 1.8 MeV $^3He^+$ beams were used. The morphology of the surfaces was inspected by scanning electron microscopy (SEM) and the formation of new phases was identified by grazing XRD and photoelectron spectroscopy (XPS). Additional details of the analytical methods and experimental apparatus are described elsewhere [12-14].

3. Results and discussion (969 words)

Figure 1 exemplifies the analytical procedure used to evaluate the elemental depth composition of the samples implanted by D^+ ions making use of the RBS and NRA techniques. The Si and W backscattered profile yields are well resolved in the RBS spectra obtained from $^4He^+$ ion beams (figure 1a), whereas RBS backscattered yields for lighter elements become highly enhanced by using incident H^+ beams [11]. All the received as-deposited samples presented elemental depth contents close to the nominal compositions. Figure 1.b exemplifies the analytical procedure used for D quantification involving the $D(^3He,p)^4He$ nuclear reaction. Simultaneously, protons emitted peaks from the

${}^9\text{Be}({}^3\text{He},\text{p}){}^{11}\text{B}$ reaction appears at lower energies in samples containing Be. Table 1 resumes the results obtained for each sample before and after D implantation for the coating thickness and for the medium composition and areal density of the retained D in the implantation zone. In the present study and in opposition with other published data, D retention does not follow the Be content in the samples, while it is much lower in the coatings presenting a Be:W ratio of (5:5). The origin of this result becomes evident from the SEM analysis performed to the entire set of samples. Figure 2a proves that the Be:W (1:9) as-deposited surface is rough and this is also the case for pure Be or W before and after D implantation (figure 2b). Moreover, the superficial roughness in the pure Be sample increases under irradiation. By the contrary, the Be:W (5:5) surfaces are extremely flat before (figures 2c) and after D implantation (figure 2d), leading to a much lower retention behaviour at $1\text{e}17\text{ D}^+/\text{cm}^2$, and additionally, it decreases after irradiation at $5\text{e}17\text{ D}^+/\text{cm}^2$, which may be easily justified by a smooth superficial erosion caused by sputtering. In resume, our results suggest that the retention mechanism depends of the surface topography.

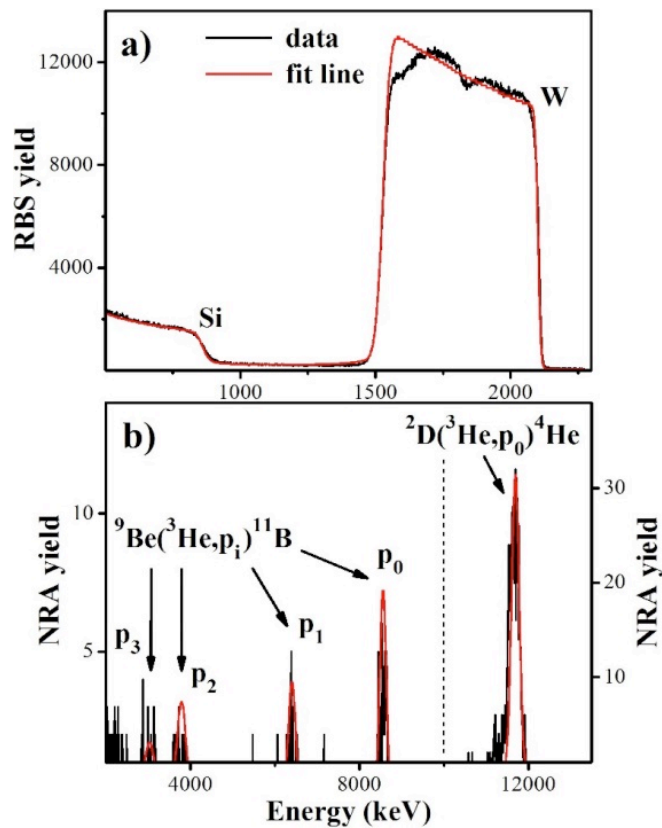


Figure 1. Analysis of a Be:W (1:9) film after $15\text{ keV } 5\text{e}17\text{ D}^+/\text{cm}^2$ exposure: RBS (1.a) and NRA (1.b) spectra collected with $2.2\text{ MeV } {}^4\text{He}^+$ and $1.8\text{ MeV } {}^3\text{He}^+$ ion beams, respectively.

Table 2 presents the analytical RBS results obtained from the N irradiation campaign. In spite of the similarity in the retained contents of both impurities in the exposed samples, the atomic fraction of N in the implantation zone is always much higher than the equivalent results for D, while the energy loss of the impinging ions inside Be or W is higher for the case of $30\text{ keV } \text{N}^+$ rather than $15\text{ keV } \text{D}^+$. As a consequence and as example, the simulated depth range (R_p) and straggling (ΔR_p) for both ions in pure Be are 84 and 21 nm and 255 and 47 nm, respectively [9]. Due to the N reactivity, almost all the impinging N ions become retained in the pure Be coating. For the same reason, the increment of N in the implantation zone also results in a Be enrichment and in the decrease of the W contents. Nevertheless, a

last and important result is the presence of a significant N amount quantified from the pure W sample. The result is in accordance with the diffractograms of figure 3.

Table 1. Thickness and elemental composition of the implantation zone in the Be:W films after D^+ exposure. The remaining elemental content relates to Oxygen (estimated error of 5 %).

Be:W film	Thick.	Be	W	D	D	
(D^+ /cm ²)	(nm)	(at.%)	(at.%)	(1e17at/cm ²)	(1e17at/cm ²)	
Be	as-dep.	832	100	0.0	-	
	1e17	838	95.4	0.0	2.81	1.19
	5e17	812	89.0	0.0	9.20	3.90
Be:W (5:5)	as-dep.	373	50.2	46.8	-	-
	1e17	366	48.8	45.8	2.33	0.43
	5e17	311	49.2	46.3	1.59	0.32
Be:W (1:9)	as-dep.	376	15.0	85.0	-	-
	1e17	399	14.2	80.7	5.10	0.88
	5e17	438	13.2	74.7	12.1	1.51
W	as-dep.	426	0.0	100.0	-	-
	1e17	453	0.0	91.4	8.30	0.79
	5e17	474	0.0	83.1	16.9	1.59

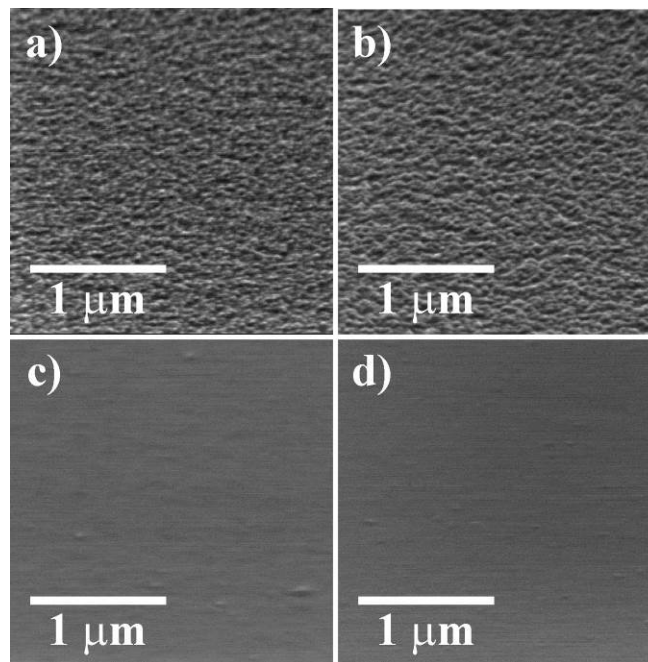


Figure 2. SEM images of an as-deposited surface with a Be:W ratio of 1:9 (2a) and after $5e17 D^+$ /cm² exposure (2b); equivalent images for an as-deposited sample presenting a Be:W ratio of 5:5 (2c) and after $5e17 D^+$ /cm² exposure (2d).

Figure 3a presents the diffractograms obtained from a pure Be coating, before and after 30 keV N^+ implantation with nominal fluences of 1 and $5e17 D^+$ /cm². It is hard to identify the presence of (pure and light) Be. Nevertheless, it is visible by the characteristic peak lines at 45.8° , 50.9° , 52.8° and 70.8° , corresponding to the diffraction pattern at planes (100), (002), (101) and (102). After irradiation at $5e17 N^+$ /cm², a new broad peak line becomes visible, as it was confirmed from an additional XRD scan at the same angular range, confirming the presence of a nitride component, possibly the β -Be₃N₂ phase at 37.1° (004) and 37.7° (101), while the peak is deviated from the

characteristic line for α -Be₃N₂ at 38.3° (222). The presence of a W component in Figure 3.b hinders the Be₃N₂ pattern. For the as-deposited Be:W (5:5) coating (Figure 3b) we identify the characteristic W pattern at 40.3° (110), 58.3° (200) and 73.2° (211), and after 5e17 N⁺/cm² exposure a β -W₂N pattern is identified at 37.8° (111), 43.9° (200) and 63.9° (220). The W and β -W₂N phases are also identified in the diffractograms related to Be:W (1:9) (figure 3c), and to pure W (figure 3d). The W pattern is also more intense now. As a consequence, we are more sensitive to its changes.

Table 2. Thickness and elemental composition of the implantation zone in the Be:W films after N⁺ exposure. The remaining elemental content relates to Oxygen (estimated error of 5 %).

Be:W film	Thick.	Be W N			N	
		(N ⁺ /cm ²)	(nm)	(at.%)		(1e17at/cm ²)
Be	as-dep.	535	94.2	0.0	-	-
	1e17	523	68.0	0.0	15.0	1.05
	5e17	569	44.1	0.0	44.1	4.25
Be:W (5:5)	as-dep.	310	54.1	37.1	-	-
	1e17	314	47.4	38.8	13.8	0.83
	5e17	332	45.0	20.0	35.0	2.63
Be:W (1:9)	as-dep.	255	8.0	92.0	-	-
	1e17	276	6.9	79.3	13.8	0.58
	5e17	292	18.0	40.0	42.0	2.18
W	as-dep.	299	0.0	100	-	-
	1e17	330	0.0	87.0	13.0	0.47
	5e17	340	0.0	60.0	40.0	1.80

In both diffractograms and after a fluence of 1e17 N⁺/cm², a new diffraction line for the W plane (110) appears at a lower (2 θ) angle close to 38.7°. From the Bragg's law, and considering the wavelength of 0.154 nm for the Cu K_α line of the X-ray source, the angular deviation corresponds to a larger lattice parameter (a') close to 0.329 nm, evidencing the formation of the W(N) solid solution phase imposed by the N implantation. For pure W and from the experimental results, the corresponding lattice parameter (a) is 0.316 nm. Thus, the increment for the modified BCC W(N) structure is about $\Delta a/a \cong 4.0\%$. At a fluence of 5e17 N⁺/cm² the new peak vanishes and give rise to the β -W₂N pattern, while β -W₂N has a more compact FCC structure. The intensities of the β -W₂N peaks in the diffractograms of Figures 3c and 3d are lower relatively to figure 3b, which may be justified by a low N content (table 2) in the samples or by a lower size of β -W₂N grains.

The presence of a W₂N phase inhibits the identification of lighter Be₃N₂ by XRD. However, it may be achieved by XPS. In agreement to the published, new XPS measurements show a slight increment of the W4f doublet binding energies [4], by increasing the incident N fluence from 1 to 5e17 N⁺/cm² in the W and Be:W (1:9) compositions, evidencing the formation of the W nitride phase [5]. A similar shift is also observed in the Be 1s binding energies for the Be and Be:W (5:5) compositions, in agreement to the formation of Be nitride [3].

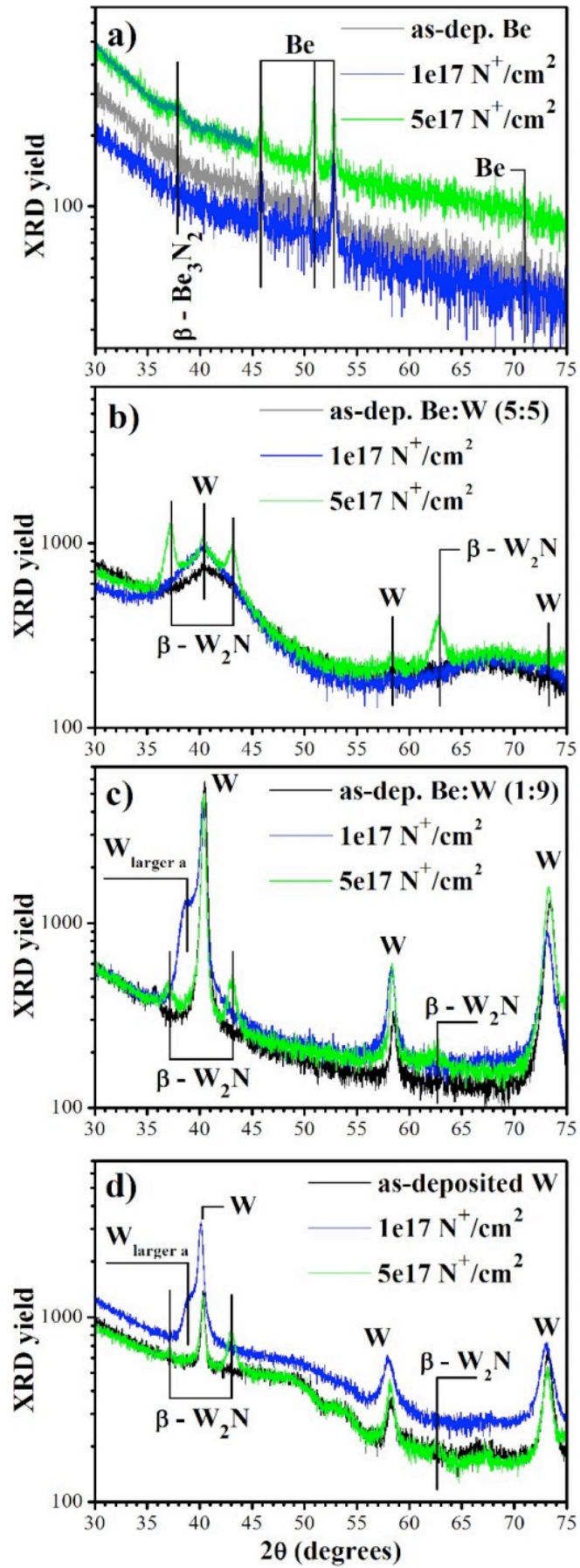


Figure 3. X-ray diffractograms collected from the entire Be:W batch after the N irradiation campaign.

4. Conclusions (88 words)

Besides the Be content, the present work have showed that hydrogen retention mechanisms seems to depend a lot of the superficial morphology of the Be:W coatings, while flat surfaces exhibited low retention values. Systematic experiments should be planned and carried out in order to prove this assumption. In parallel, N retention followed the Be content in the samples. Besides the Be₃N₂ phase, it was identified the formation of β-W₂N under energetic N bombardment. It will be interesting to evaluate the stability of the phase at higher temperatures [4].

Acknowledgements (57 words)

This work has been carried out within the framework of the of the EUROfusion Consortium and has received funding from the European Union's Horizon 2020 research under grant agreement number 633053 and from "Fundação para a Ciência e Tecnologia" through project Pest-OE/SADG/LA0010/2013. The views and opinions expressed herein do not necessarily reflect those of the European Commission.

References (147 words)

- [1] Wright G M et al 2010 *Nucl. Fusion* 50 055004
- [2] Oberkofler M et al 2011 *Nucl. Instrum. Meth. B* 269 1266
- [3] Oberkofler M and Linsmeier Ch 2010 *Nucl. Fusion* 50 125001
- [4] Schmid K et al 2010 *Nucl. Fusion* 50 025006
- [5] Oberkofler M et al 2013 *J. Nucl. Mater.* 438 S258
- [6] Ropp R C 2013 *Encyclopedia of the Alkaline Earth Compounds* (Amsterdam, Elsevier)
- [7] Kieffer R and Benesovsky F 1963 *Hartstoffe* (Wien, Springer-Verlag)
- [8] Lungu C P et al 2007 *Phys. Scr.* T128 157
- [9] SRIM 2013 software package, <http://www.srim.org>
- [10] Cullity B D 1978 *Elements of X-ray Diffraction*, second ed. (Reading, Massachusetts, Addison-Wesley)
- [11] IBANDL data library, IAEA, 2014 at <http://www-nds.iaea.org/ibandl/>
- [12] Mateus R et al 2013 *J. Nucl. Mater.* 432 S1032
- [13] Mateus R et al 2013 *J. Nucl. Mater.* 442 S320
- [14] G. Schinteie et al *J. Nucl. Mater.* 457 (2015) 220